

Size-Dependent Switching of the Spatiotemporal Structure between a Traveling Wave and Global Rhythm

Ryoichi Aihara^{†,‡} and Kenichi Yoshikawa^{*,§}

Graduate School of Human Informatics, Nagoya University, Nagoya 460-8601, Japan, Bio-Mimetic Control Research Center, The Institute of Physical and Chemical Research (RIKEN), Nagoya 463-0003, Japan, and Department of Physics, Graduate School of Science, Kyoto University & CREST, Kyoto 606-8502, Japan

Received: March 8, 2001; In Final Form: June 20, 2001

The spatiotemporal chemical structure in the Belousov–Zhabotinsky (BZ) reaction was studied using spherical beads of ion-exchange resin doped with ferroin by changing the size of the beads. Above an upper critical size (ca. 0.8 mm in diameter), chemical waves emerge and propagate on the surface of a bead by forming a target or spiral pattern. Below a lower critical size (ca. 0.62 mm in diameter), uniform global oscillation over the entire bead is observed; i.e., no traveling wave is observed. Between these upper and lower critical sizes, the reaction is bistable with regard to the two different modes, i.e., uniform oscillation and a traveling wave. This experimental trend is discussed in terms of competition between the growth rate and diffusion rate of the activator.

Introduction

Oscillatory chemical reactions have attracted much interest as being representative of spatiotemporal self-organization under thermodynamically open conditions. Among such oscillatory chemical systems, the Belousov–Zhabotinsky (BZ) reaction is the most famous.^{1,2} This oscillatory reaction was discovered by Belousov when he was studying chemical reactions in aqueous solution as a model of the cytoplasmic metabolism of natural organic acids.³ Thus, the BZ reaction is considered an *in vitro* model of living matter. Exotic spatiotemporal structures, such as target and spiral patterns and Turing instability, have been observed in actual experiments on the BZ reaction and its modifications.^{4–7} Most of the experiments on the spatiotemporal structures in the BZ reaction have been performed for systems at a scale larger than 1 cm. This may be due to the ease of experimental handling and visual observation. On the other hand, the scale of living cells is much smaller than 1 cm. Thus, it may be useful to examine the effect of a small volume on an oscillatory chemical reaction. The purpose of this study was to investigate the effect of the spatial scale on spatiotemporal structures by adapting the BZ reaction as a typical nonlinear dynamical system in chemistry.

Maselko and Showalter observed the generation and propagation of a spiral wave on the surface of single spherical beads 0.5–1.4 mm in diameter and loaded with ferroin.⁸ Nishiyama studied the coupling between bead oscillators 0.07–0.15 mm in diameter, where individual beads exhibit homogeneous oscillation instead of generating a traveling wave.^{9,10} It has also been reported that homogeneous oscillation is observed in the BZ reaction with ion-exchange beads 0.2–0.8 mm in diameter.¹¹ In this experiment, the oscillation frequency decreased with a decrease in the size of the beads, which was attributed to escape

of the activator HBrO₂ through the interface. In a summary of these current studies on the finite-size effect in the BZ reaction, it is clear that a traveling wave is generated for systems larger than about 1 mm, whereas homogeneous global oscillation is observed for smaller systems. However, there seems to have been no systematic study on the size in the transition of the spatiotemporal structure between a traveling wave and homogeneous global oscillation. In this study, we investigated the BZ reaction in isolated ion-exchange resin beads doped with ferroin, with special attention on the effect of the size of beads ranging from 0.1 to 1.3 mm in diameter.

Experimental Section

The experiments were performed for isolated beads bathed in aqueous BZ solution without catalyst. The oscillatory reaction proceeds only on beads doped with catalyst. Ferroin solutions were prepared from 1,10-phenanthroline and iron(II) sulfate heptahydrate (Wako Pure Chemical Industries, Ltd.). Sulfuric acid and molonic acid were obtained from Wako Pure Chemical Industries, Ltd., and sodium bromate was from Nacalai Tesque. The cation-exchange resin (Dowex 50W-X4) loaded with ferroin was prepared by mixing 1 g of beads with 10 mL of ferroin solution [$[\text{Fe}(\text{phen})_3^{2+}] = 3.6 \times 10^{-3} \text{ M}$] and then stirring gently for 1 h. All measurements were carried out at 23 °C. All observations were made on a Petri dish (5 cm in a diameter) under a microscope (DIAPHOT-TMD, Nikon) and monitored with a CCD camera (CCD-S1, Shimadzu). Experimental images were processed by subtracting each image from the time-average signal as a background.¹²

Results

Figure 1 shows the time evolution of the spatial pattern on spherical beads with a diameter of 1.03 mm, together with a snapshot of the whole view, (a) just after the start of the experiment and (b and c) after 90 min. The beads loaded with

* To whom correspondence should be addressed. E-Mail: yoshikaw@sphys.kyoto-u.ac.jp.

[†] Nagoya University.

[‡] The Institute of Physical and Chemical Research (RIKEN).

[§] Kyoto University & CREST.

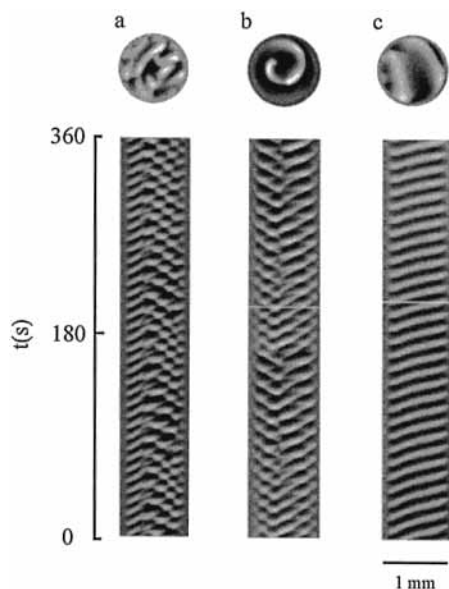


Figure 1. Spatiotemporal chemical pattern observed on spherical beads with a diameter of 1.03 mm after (a) 30 min, (b) 90 min, and (c) 100 min after the start of the experiment. The upper pictures are snapshots of the propagation of traveling waves. The lower pictures are space–time diagrams.

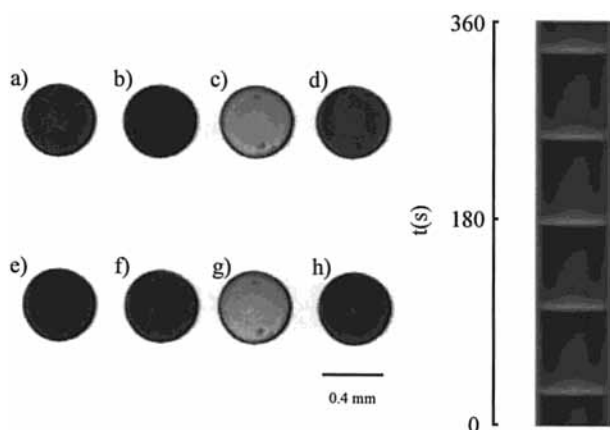


Figure 2. Global uniform rhythm observed on spherical beads with a diameter of 0.41 mm. The time interval for (a)–(h) is 22 s.

ferroin were placed in a Petri dish containing BZ solution to a depth of 5 mm. The spatiotemporal change in the BZ reaction is observed as a change in the intensity of transmitted light. At the initial stage of the experiments, chemical waves tended to be generated in a random manner, as in Figure 1a. After several tens of minutes, however, a stable spiral wave prevails over the entire surface of the bead, as in Figure 1b (front view) and Figure 1c (side view). These characteristic spiral waves are generated in a stationary manner for up to several hours. Similar spiral waves have been observed on bead oscillators (0.5–1.4 mm in diameter) by Maselko and Showalter.⁸

Figure 2 shows the oscillation in a bead with a diameter of 0.41 mm. The spatiotemporal diagram on the right in Figure 2 clearly indicates the all-or-none nature of the firing over the bead; i.e., the oscillation is homogeneous the bead. Similar homogeneous global oscillation has been reported by Nishiyama for beads with diameter of 0.07–0.15 mm.^{9,10}

The results of observations for behavior are summarized in Figure 3. Depending on the diameter, two types of space–time behavior are observed. The propagation of chemical waves is always observed for beads larger than 0.81 mm in diameter,

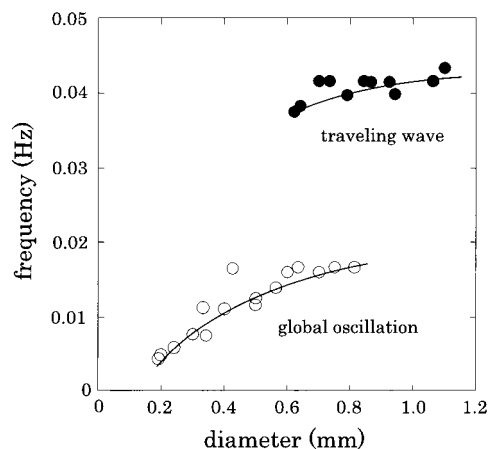


Figure 3. Dependence of frequency on the bead diameter for the two different modes of oscillation: closed circle, traveling wave; open circle, homogeneous oscillation.

and uniform rhythm is always observed below 0.62 mm. For the intermediate region of 0.62–0.81 mm, chemical waves tend to appear for the initial several minutes and then are replaced by a uniform global rhythm. No chemical wave is generated for beads less than 0.6 mm in diameter, even though the characteristic width of the wave front (ca. 0.1 mm) is much smaller than the diameter of the bead. The decrease in the oscillatory frequency with a decrease in size, as shown in Figure 3, is attributable¹¹ to the escape of the activator from the surface of the beads, being different from the experiments on larger experimental systems above the size of 1 mm.

Discussion

It is well-known that the spatiotemporal structure in a reaction–diffusion system is usually insensitive to the boundary condition or to the size or shape of the field.^{13,14} This may be true for any system larger than approximately 1 cm. On the other hand, the present results clearly show that the mode of spatiotemporal pattern formation switches at a diameter of around 0.6–0.8 mm.

We now discuss why size has such a significant effect in a system smaller than 1 mm. As for the kinetics of simple diffusion, the diffusion length, l , is roughly proportional to the square of time, t .

$$l \sim \sqrt{Dt} \quad (1)$$

The diffusion constant D is only weakly dependent on the molecular weight M , $D \propto M^{1/3}$, and is on the order of 10^{-5} cm²/s in usual aqueous solution. In contrast, a traveling wave in a reaction–diffusion system exhibits a constant speed as it propagates in a stationary solution. Thus, the traveling length, l , is given as

$$l = c_p t \quad (2)$$

where c_p is the velocity. Therefore, it is apparent that simple “diffusion” is important over a short time scale. A crossover of the two kinetic processes, simple diffusion and wave propagation, will occur at the critical length l_c , as shown in Figure 4.

$$l_c \sim D/c_p \quad (3)$$

Let us estimate the change in the effective diffusion constant within the bead reactor. On the basis of the experimental observation of large beads, as in Figure 1, the velocity and

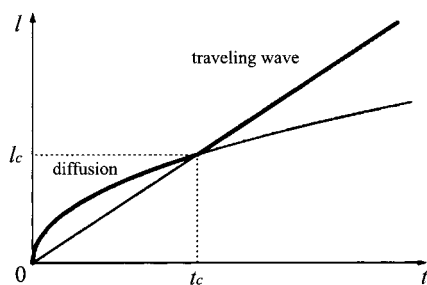


Figure 4. Schematic representation of the competition between simple diffusion (eq 1) and a traveling wave (eq 2).

propagation frequency can be estimated to be $C_{\text{bead}} \approx 0.04$ mm/s and $f_{\text{bead}} \approx 0.04$ Hz, respectively. It has been well established that, in BZ medium, the wave velocity is roughly proportional to the square root of the diffusion constant, $c \propto \sqrt{k_5 D}$,¹⁵ and that the reaction rate constant k_5 is roughly proportional to the frequency, f , where k_5 is the rate constant for the autocatalytic process of an Oregonator. On the basis of this consideration, the diffusion constant of the activator in the bead is given as

$$D_{\text{bead}} \approx D_{\text{aq}} \left(\frac{c_{\text{bead}}}{c_{\text{aq}}} \right)^2 \frac{k_{5,\text{aq}}}{k_{5,\text{bead}}} \approx D_{\text{aq}} \left(\frac{c_{\text{bead}}}{c_{\text{aq}}} \right)^2 \frac{f_{\text{aq}}}{f_{\text{bead}}} \quad (4)$$

The diffusion constant of a low-molecular-weight species in aqueous solution, D_{aq} , is 2×10^{-5} cm²/s.¹⁶ We measured the traveling waves on BZ medium in the absence of beads under the same chemical conditions and found that the velocity and frequency are $c_{\text{aq}} \approx 0.06$ mm/s and $f_{\text{aq}} \approx 0.05$ Hz, respectively. Thus, D_{bead} should be around 1.1×10^{-5} cm²/s. The critical length on the bead reactor is now estimated to be $l_c \sim 0.03$ mm. This critical length is 1 order of magnitude smaller than that observed in the experiment (Figure 3).

To gain further insight into the mode-switching between traveling wave and global oscillation, we performed numerical simulations on a two-variable Oregonator:¹⁷

$$\begin{cases} \frac{\partial u}{\partial t} = \frac{1}{\epsilon} \left(u - u^2 - \frac{fv(u - \mu)}{u + \mu} \right) + D_u \nabla^2 u \\ \frac{\partial v}{\partial t} = u - v \end{cases} \quad (5)$$

Here the variables u and v correspond to the dimensionless concentrations of HBrO₂ and Fe(phen)₃³⁺, respectively. Since the catalyst is immobilized on the beads in our experiment, neglecting the diffusion of v should give a reasonable approximation. The parameters are $\epsilon = 0.01$, $f = 2$, $\mu = 0.002$, and $D_u = 1$.¹⁸ To interpret the chemical dynamics in the bathing solution in the absence of the catalyst, we adapt the following equation:¹⁹

$$\frac{\partial u}{\partial t} = -\frac{1}{\epsilon} u^2 + D_u \nabla^2 u \quad (6)$$

Here the first term on the right corresponds to the disproportionation reaction. The one-dimensional reaction–diffusion field (eq 5) is related to the diffusion field (eq 6) on both sides. Integration is carried out by a fourth-order Runge–Kutta algorithm with a time step of $\Delta t = 0.01$ and on 480 arrays with no-flux boundary conditions at both ends.

To investigate the effect of the system size, the size is scaled as

$$(x, y, z) \rightarrow (\xi x, \xi y, \xi z) \quad (7)$$

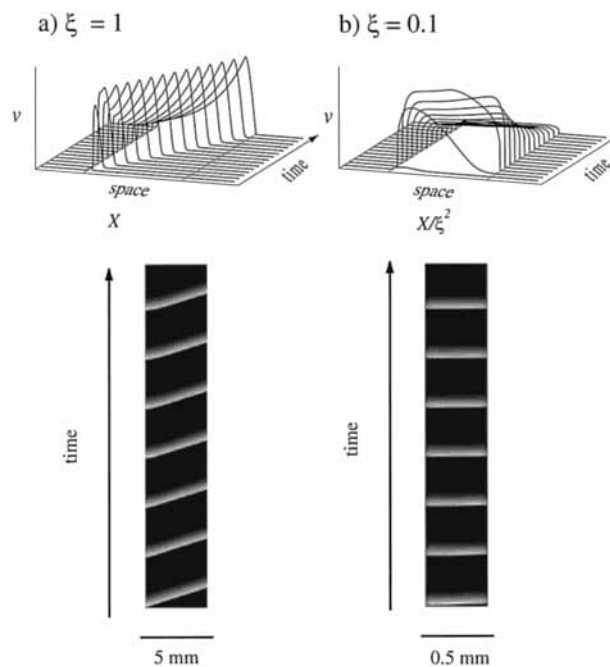


Figure 5. Time evolution of the concentration profile of the inhibitor v calculated from eqs 8 and 9 for different spatial scales (a) $\xi = 1.0$ and (b) $\xi = 0.1$. The parameters are $\epsilon = 0.01$, $f = 2$, $\mu = 0.002$, and $D_u = 1$. Time dependence in a one-dimensional field is given where the left edge shows an increase in v at $t = 0$. The bottom pictures are the space–time diagrams for the same numerical calculation.

Accordingly, eqs 5 and 6 are converted to

$$\begin{cases} \frac{\partial u}{\partial t} = \frac{1}{\epsilon} \left(u - u^2 - \frac{fv(u - \mu)}{u + \mu} \right) + \frac{D_u}{\xi^2} \nabla^2 u \\ \frac{\partial v}{\partial t} = u - v \end{cases} \quad (8)$$

and

$$\frac{\partial u}{\partial t} = -\frac{1}{\epsilon} u^2 + \frac{D_u}{\xi^2} \nabla^2 u \quad (9)$$

respectively. The parameter ξ is introduced to take into account the effect of the system size with the same precision, or the same mesh number, on the numerical simulation. To gain insight into the essence of the size effect, we have performed the simulation on one-dimensional system. This is partly due to the difficulty in performing precise numerical simulation with eq 8 for a large system as in a three-dimensional object.

Figure 5a,b shows the time evolution of v in a spatially one-dimensional system with $\xi = 1$ and 0.1 , respectively, where the time evolution of the inhibitor after the application of a small perturbation ($\Delta u = 0.002$) to the edge of the reaction–diffusion field is shown. With reference to the scaled variables, the results of Figure 5a,b correspond to actual sizes of 4.3 and 0.43 mm, respectively. Figure 5a shows the appearance of a fully developed traveling wave propagating from left to right, whereas Figure 5b shows the generation of almost homogeneous global oscillation. As shown on profiles of the inhibitor in the numerical simulation in Figure 5b, diffusion is faster than the growth of the chemical wave, due to the small size of the system. Thus, the space–time diagrams in Figure 5a,b agree well with the experimental results in Figures 1c and 2, except for the marked change in the frequency in Figure 5b. Here, it is to be mentioned that the difference in the reaction condition between the inner and outer regions in the spherical beads will also cause a

nonnegligible effect on the manner of oscillation. For example, the failure of the simulations to show a marked decrease in periodicity with a decrease in size would be due to the difference in the spatial dimensionality between the experiment with bead oscillators (three-dimensional) and the numerical simulations (one-dimensional).

Conclusion

We studied the size dependence of the spatiotemporal pattern in the BZ reaction, occurring on spherical beads. Our results have shown that, with a decrease in the size of the system, the spatiotemporal pattern switches from a traveling wave to uniform global oscillation. This switching is induced as a result of competition between the growth rate of the chemical wave and diffusion. Such mode-switching in the spatiotemporal pattern may be of interest for comparison with spatiotemporal structures in living cellular systems.

Acknowledgment. We thank Ms. I. N. Motoike for numerical programming. This work has been supported in part by a Grant-in-Aid from the Ministry of Education, Culture, Sports, Science, and Technology of Japan.

References and Notes

(1) Field, R. J., Burger, M., Eds. *Oscillations and Traveling Waves in Chemical Systems*; Wiley: New York, 1985; p 1.

(2) Kapral, R., Showalter, K., Eds. *Chemical Waves and Patterns*; Kluwer: Dordrecht, The Netherlands, 1994.

(3) Zhabotinsky, A. M. In *Oscillations and Traveling Waves in Chemical Systems*; Field, R. J., Burger, M., Eds.; Wiley: New York, 1985, p 1. Belousov, B. P. In *Oscillations and Traveling Waves in Chemical Systems*, Field, R. J., Burger, M., Eds.; Wiley: New York, 1985; p 605.

(4) Zaikin, A. N.; Zhabotinsky, A. M. *Nature* **1970**, 225, 535.

(5) Winfree, A. T. *Science* **1972**, 175, 634.

(6) Castets, V.; Dulos, E.; Boissonade, J.; De Kepper, P. *Phys. Rev. Lett.* **1990**, 64, 2953.

(7) Ouyang, Q.; Swinney, H. L. *Nature* **1991**, 352, 610.

(8) Maseko, J.; Showalter, K. *Nature* **1989**, 339, 609.

(9) Nishiyama, N.; Eto, K. *J. Chem. Phys.* **1994**, 100, 6977.

(10) Nishiyama, N. *Physica D* **1995**, 80, 181.

(11) Yoshikawa, K.; Aihara, R.; Agladze, K. *J. Phys. Chem. A* **1998**, 102, 7649.

(12) Miike, H.; Zhang, L.; Sakurai, T.; Yamada, H. *Pattern Recognit. Lett.* **1999**, 20, 451.

(13) Ross, J.; Müller, S. C.; Vidal, C. *Science*. **1988**, 240, 640.

(14) Swinney, H. L., Krinsky, V. I., Eds. *Waves and Patterns in Chemical and Biological Media*; *Physica D* **1991**, 49, 1–2.

(15) Tyson, J. In *Oscillations and Traveling Waves in Chemical Systems*; Field, R. J., Burger, M., Eds.; Wiley: New York, 1985; p 93.

(16) Murray, J. D. *Mathematical Biology*; Springer-Verlag: Berlin, 1993.

(17) Keener, J. P.; Tyson, J. J. *Physica D* **1986**, 21, 307.

(18) Jahnke, W.; Winfree, A. T. *Int. J. Bifurcat. Chaos* **1991**, 1, 445.

(19) Kusumi, T.; Yamaguchi, T.; Aliev, R. R.; Amemiya, T.; Ohmori, T.; Hashimoto, H.; Yoshikawa, K. *Chem. Phys. Lett.* **1997**, 271, 355.